Pauli Shielding and Breakdown of Spin Statistics in Multielectron Multi-Open-Shell Dynamical Atomic Systems

I. Madesis, A. Laoutaris, and T. J. M. Zouros*
Department of Physics, University of Crete, GR-70013 Heraklion, Greece
and Tandem Accelerator Laboratory, Institute of Nuclear and Particle Physics, NCSR "Demokritos", GR-15310 Agia Paraskevi, Greece

E. P. Benis
Department of Physics, University of Ioannina, GR-45110 Ioannina, Greece

J. W. Gao
Institute of Applied Physics and Computational Mathematics, 100088 Beijing, China,
Laser Fusion Research Center, China Academy of Engineering Physics, 621900 Mianyang, China
and Sorbonne Université, CNRS, Laboratoire de Chimie Physique-Matière et Rayonnement, F-75005 Paris, France

A. Dubois†
Sorbonne Université, CNRS, Laboratoire de Chimie Physique-Matière et Rayonnement, F-75005 Paris, France

(Received 23 December 2019; revised manuscript received 10 February 2020; accepted 22 February 2020; published 20 March 2020)

We report on $C^{3+}(1s2\ell 2\ell'\,^{2S+1}L)$-resolved cross sections of electron capture in collisions of swift $C^{4+}(1s2s\,^3S)$ ions with helium and hydrogen. The study focuses on the formation of doubly excited triply open-shell $C^{3+}(1s2s2p)\,^4P$ and $^2P_\pm$ states with emphasis on the ratio R of their cross sections as a measure of spin statistics. Using zero-degree Auger projectile spectroscopy and a three-electron close-coupling semiclassical approach, we resolve a long-standing puzzle and controversy on the value of R and on the effect of cascades, to clarify the underlying physics. The present results invalidate the frozen core approximation generally used in the past when considering electron capture in multielectron multi-open-shell quantum systems. A distinctive screening effect due to the Pauli exclusion principle (Pauli shielding) is proposed to account for the value of R, consistent with our findings.

DOI: 10.1103/PhysRevLett.124.113401

The dynamics of excited atomic or molecular structures with several unpaired electrons is complex to understand and theoretically model due to the interplay of several fundamental aspects of atomic physics: rich spectral signatures involving multiple spin symmetries, electronic correlation, and intricate reactivity sketched by numerous open channels, all under the constraints of the Pauli exclusion principle. High energy few-electron ions in collision with atomic targets provide one of the simplest benchmark quantum systems to probe the underlying physics at the most fundamental level. Their atomic line spectra excited in collisions with electrons, ions, or atoms provide important information about the atomic structure of the observed states, as well as their basic production mechanisms [1,2]. In particular, state-resolved x-ray [3] and Auger electron [4] measurements provide the most stringent tests of this understanding, finding important practical applications in various fields of astrophysical [2,5] and laboratory [5,6] plasmas.

Here, we revisit the long-standing problem of how multi-unpaired-electron ion cores behave while undergoing electron processes during fast atomic collisions, and how best to accurately describe them theoretically. Previous work on ionization [7,8], excitation [9,10], and electron loss [11] have shown that important dynamic electron correlations involving higher-order processes such as time ordering and Pauli blocking need to be considered, once one goes beyond the independent electron and frozen core approximations. However, for single electron capture (SEC) involving multi-open-shell excited ions, the situation is much less clear [12]: (i) Are similarly configured final states corresponding to different spins populated according to spin statistics? (ii) How legitimate is the frozen core approximation or, equivalently, does the initial electronic configuration undergo changes during the collision process?

A viable way to explore these issues is to consider the following $2p$ SEC channel in MeV collisions:

$$C^{4+}(1s2s\,^3S) + He \rightarrow C^{3+}(1s2s2p\,^4P,\,^2P_\pm) + He^+, \quad (1)$$

which can be readily investigated experimentally since the initial, $1s2s\,^3S$, ionic core is metastable and therefore

naturally found mixed in with the ground state ions as provided by accelerators [15–17]. Then, the ratio R of the $1s2s2p\ ^4\mathrm{P}/^2\mathrm{P}_\pm$ SEC cross sections,

$$R = \frac{\sigma(^4\mathrm{P})}{\sigma(^2\mathrm{P}_+) + \sigma(^2\mathrm{P}_-)}, \tag{2}$$

could bear the corresponding population spin statistics signature. Indeed, this ratio results in $R = 1$, when considering only spin multiplicity [18], while $R = 2$ in the frozen core approximation where only the ^{4}P and a single ^{2}P can be produced from the $1s2s\ ^3$S initial state [19,20]. Such statistical arguments and approximations are often used to simplify difficult problems of computing relative populations in high energy plasmas [2] and can therefore be of important practical use.

It was therefore particularly intriguing when Tanis *et al.* [21] reported a larger value $R \simeq 2.9$, in 20.9 MeV collisions between mixed-state $\mathrm{F}^{7+}(1s^2\ ^1\mathrm{S}, 1s2s\ ^3\mathrm{S})$ ions and He. This led these authors to propose a new mechanism, the dynamic Pauli exchange interaction, to explain the preponderance of $1s2s2p\ ^4$P state over the $1s2s2p\ ^2\mathrm{P}_\pm$ states populations. Alternatively, Zouros *et al.* [22], showed that a similar enhancement of R could also be qualitatively explained by a *selective* cascade feeding mechanism favoring the ^{4}P production. As a consequence, in both schemes, the measured ratio R does not directly reflect simple final state spin statistics.

In a more detailed follow-up investigation of the process in Eq. (1), even larger experimental ratios $R \simeq 6$–9 were reported [20]. In addition, calculations based on a frozen core single-active electron treatment were included using the nonperturbative basis generator method (TC-BGM) [23,24], with a detailed radiative cascade analysis [20], and additional Auger corrections [25]. These authors clearly demonstrated a selective cascade enhancement of the ^{4}P state, resulting in $R \simeq 4.9$–5.8 [20,25]. Yet, for just $2p$ capture (no cascades), the computed values were found to give $R = 2$ [25], the spin statistics prediction within the frozen core approximation, resulting in a rather puzzling paradoxical situation.

In this Letter, we treat this problem both theoretically and experimentally for the electron capture processes of Eq. (1) induced in 2–18 MeV collisions of $\mathrm{C}^{4+}(1s2s\ ^3\mathrm{S})$ ions with helium and hydrogen targets. We perform intensive close-coupling calculations involving the dynamics of three active electrons [26]. The ratio R, stemming from this treatment and the inclusion of cascade effects, is compared to our measurements using the recent two-spectra technique [27,28] to directly extract the contributions from just the metastable component. For the first time, agreement between theory and experiment is found. This resolves the long-standing paradox, while revealing the existence of novel strong electron correlation effects, not included in previous treatments, primarily due to their intrinsic one-active-electron limitations.

The measurements were performed with the zero-degree Auger projectile spectroscopy (ZAPS) [29] setup [30] currently located at the NCSR "Demokritos" 5.5 MV Tandem accelerator facility, which delivered the He-like C^{4+} ion beams. The electron spectrometer consists of an electrostatic single stage hemispherical deflector analyzer equipped with a four-element injection lens and a 2D position sensitive detector (PSD) [31]. High statistics spectra were recorded with sufficient resolution to clearly separate the C^{3+} KLL Auger lines by preretarding the measured electrons by a factor of 4, while also exploiting the high efficiency afforded by our multichannel PSD. Beam intensities on target ranged from 0.1–20 nA depending on incident energy and stripping conditions, while target gas pressures ranging from 5–40 mTorr were chosen to ensure single collision conditions. Using different electron stripper combinations [17,30], beams of $\mathrm{C}^{4+}(1s^2, 1s2s\ ^3\mathrm{S})$ mixed-state ions were prepared with different amounts of metastable $1s2s$ component so that the ratio R could be accurately determined by applying our two-spectra technique [27].

In Fig. 1, we present typical Auger spectra from collisions of 9 MeV mixed-state $\mathrm{C}^{4+}(1s^2\ ^1\mathrm{S}, 1s2s\ ^3\mathrm{S})$ with He and H_2. Similar spectra were also recorded at 6, 12, and 15 MeV for He, and also at 6 and 12 MeV for H_2 targets. At each collision energy, as shown in Fig. 1 for 9 MeV, two spectra were recorded, each with a different $1s2s\ ^3$S metastable fraction, as evidenced by the distinct intensities of the $1s2s2p\ ^4$P peaks [27]. Indeed, the ^{4}P state is populated almost exclusively by SEC to the $1s2s\ ^3$S state due to spin considerations [32], while the $1s2p^2\ ^2$D state is mainly produced by transfer excitation (TE) [33] from the

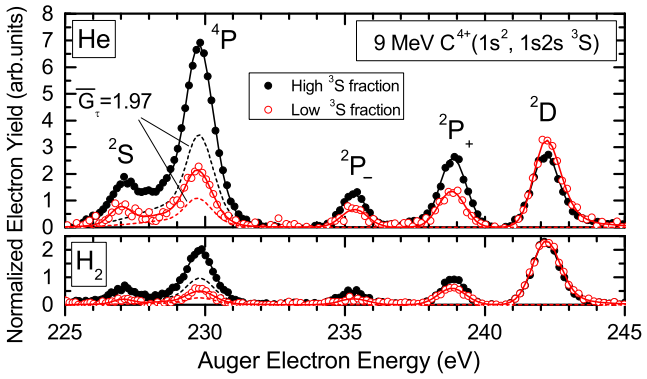

FIG. 1. Typical ZAPS C^{3+} KLL Auger spectra after background subtraction and transformation to the projectile rest frame for 9 MeV mixed state $\mathrm{C}^{4+}(1s^2, 1s2s\ ^3\mathrm{S})$ ion beam collisions with He (top) and H_2 (bottom). The states $1s2s^2\ ^2$S, $1s2s2p\ ^4$P, $1s2s2p\ ^2\mathrm{P}_-$, $1s2s2p\ ^2\mathrm{P}_+$ and $1s2p^2\ ^2$D are indicated. High (filled black circles) and low (open red circles) $1s2s\ ^3$S metastable fraction spectra are shown (see text). The true intensity of the ^{4}P line is also shown (dashed lines) after division by the indicated factor $\overline{G}_\tau$ [35,36].

$1s^2$ ground state [22,27,34] in this range of impact energies. The rest of the observed KLL states can be populated from both the ground state $1s^2$ by TE and the metastable state by SEC [22,27,32,34]. This dual spectrum measurement is the cornerstone of our recently reported technique [27] for separating out from the measured yields the contribution of just the metastable $1s2s\,^3$S beam component. Also shown in Fig. 1 is the value of the computed $\overline{G}_\tau$ intensity correction factor [29,30,35,36] applied to the detection of the delayed Auger electrons emitted at 0° to the beam direction from the long-lived $C^{3+}(1s2s2p\,^4P_J)$ J levels [37]. This important correction accounts for two competing effects: the increase in solid angle for electrons emitted from ions approaching the spectrometer, and the loss of electrons emitted from ions inside and beyond the spectrometer. In our setup, it reduces the observed intensity by about 2, depending on projectile velocity [36].

Moreover, our measurements (and calculations) highlighted the fact that higher-lying C^{3+} states are also significantly populated in the collision. This can be seen in Fig. 2, where KLn Auger lines, extending to the carbon

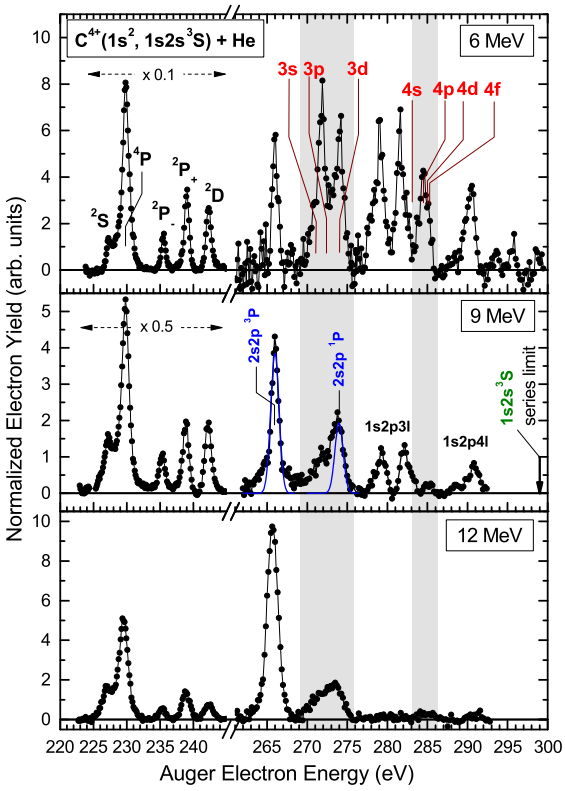

FIG. 2. ZAPS C^{3+} and C^{4+} K-Auger spectra for 6, 9, and 12 MeV collisions of mixed-state $C^{4+}(1s^2, 1s2s\,^3S)$ with He. Within the gray bands, some of the observed higher-lying $1s2sn\ell\,^2$L states are identified in red by their $n\ell$ values. Other lines labeled in black (middle panel) are the $1s2pn\ell$ doublets and do not contribute to the cascades. Indicated in blue, for completeness, are the strong $C^{4+}(2s2p)$ excitation lines. Note that the lines in the 220–245 eV domain are scaled.

$1s2s\,^3$S series limit (≃299 eV), are presented. Among others, lines from $1s2sn\ell\,^2$L states with $n = 3$ and 4 (marked $n\ell$ in the figure) are clearly observed. Indeed, these doublets are emptied very rapidly due to their strong Auger rates. This results in much reduced $E1$ radiative branching ratios [25], so that their populations never cascade to the lowest lying $1s2s2p\,^2P_\pm$. In contrast, the corresponding $1s2sn\ell\,^4$L ($n = 3, 4$) states are not observed in Fig. 2, even though they lie in the same energy range as their doublet counterparts and should be similarly populated by SEC. This absence is in fact due to their very weak Auger decay to $C^{4+}(1s^2)$ [38], forbidden due to spin conservation. Consequently, these quartets have very large $E1$ radiative branching ratios to lower lying quartets [38–40] and therefore their populations are efficiently transferred by cascades to the lowest quartet, the $1s2s2p\,^4$P state. This demonstrates that our measured ^{4}P cross sections and related R ratios arise not only from direct, genuine collision induced transfer, but also from cascades, as pointed out in the introduction.

In parallel with the experimental investigations, we have performed *ab initio* dynamical calculations involving three active electrons within a full configuration interaction approach. Our treatment is based on a semiclassical atomic orbital close-coupling approach (referred to as 3eAOCC in the following), with asymptotic descriptions of the atomic collision partners [26,41,42]: the time-dependent Schrödinger equation is solved nonperturbatively, with inclusion of all couplings related to the static and dynamic interelectronic repulsions and effects stemming from the Pauli exclusion principle. This allows for an accurate modeling of the C^{4+} and C^{3+} electronic structures, including spin and spatial components, and of their dynamics inducing, among others, excitation and capture to doubly excited states on the carbon center [43]. It therefore goes much beyond frozen core models advocated in the past [20,25], where only one active electron is considered in the dynamics. Both atomic center electronic structures are represented in terms of sets of Gaussian-type orbitals (GTO) and selected products of these GTOs, in order to obtain fully antisymmetrized, electron indistinguishable wave functions for states of singlet, doublet, triplet, and quartet spin symmetries. The GTO sets were optimized to accurately describe up to three open-shell electronic configurations with special emphasis on $C^{3+}(1s2\ell n\ell')$ for $n = 2$, 3 and ℓ, $\ell' = 0$, 1 (see Supplemental Material for details [44]). Total cross sections (after multiplying by a factor of 2 to account for the two electrons on the real targets) can then be computed for all processes spanned by the basis sets. The ratio R [Eq. (2)] is evaluated, using partial ($M_L = 0$) cross sections for the three P states under consideration, in accordance with known ZAPS sensitivity [33] to the component parallel to the impact velocity direction (defining the z axis in our calculations). Since states lying above the $C^{3+}(1s2s2p\,^{2,4}P)$ levels are present

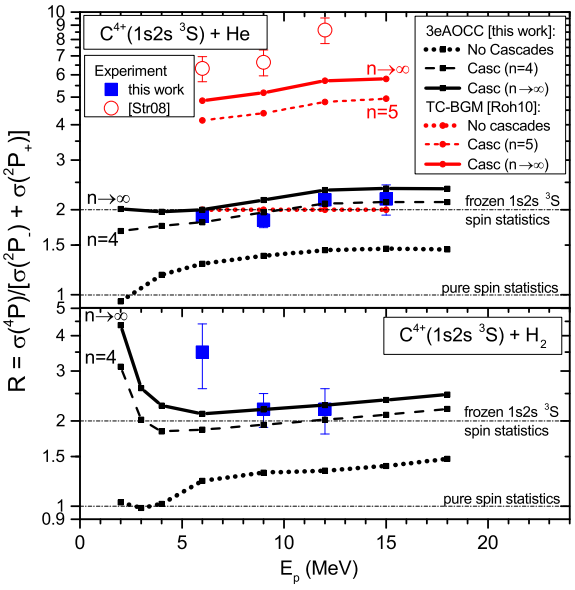

FIG. 3. Ratio R [Eq. (2)], for $C^{4+}(1s2s\,^3S)$ collisions with He (top) and H_2 (bottom) as a function of projectile energy. Experiment (ZAPS): Squares (this work), circles [20]. Theory: Black lines (3eAOCC, this work), red lines [25]. Results without (dotted) and with radiative cascades from $1s2snl\,^4L$ states up to the indicated n (dashed) and extrapolated to $n \to \infty$ (solid) are shown. The frozen $1s2s\,^3S$ core spin statistics and pure spin statistics values are also indicated.

as well in our basis sets, R was also evaluated including radiative cascade feeding within the quartet symmetry [20,22,25], in accordance with the above discussion.

In Fig. 3, we show the present results (in black lines and squares) on the ratio R for He and H_2, together with the previous independent results (in red lines and circles) for the He target [20,25], pointing out the disagreement existing to date [47]. For R evaluated theoretically, we provide three limiting cases: (i) the genuine R value (dotted lines) calculated using the $2p$ SEC cross sections stemming from the 3eAOCC calculations, and (ii) two R values taking into account radiative cascade contributions within the quartet series, in accordance with the discussion above. These two latter R values were evaluated using radiative branching ratios calculated with the COWAN code [48] and SEC cross sections to higher-lying $1s2sn\ell\,^4L$ states provided by our AOCC treatment. We then include cascades from SEC populating only the $n = 3$ and $n = 4$ quartet levels (black dashed lines) and extrapolate to include all higher quartets (black solid lines) based on an n^{-3} population model, also used previously [25]. Very good agreement with our measured R values is observed for both targets. This unambiguously demonstrates that cascades make an important contribution to the measured ratio R, increasing with decreasing impact energies, while masking the spin statistics considerations advocated in the past. Finally, the difference observed with the TC-BGM calculations [25] (red lines in Fig. 3) can be readily attributed to the present use of a dynamic approach involving several active correlated electrons, avoiding the constraints of the $1s2s\,^3S$ frozen core approximation required in one-electron treatments.

The important new understanding provided by the present 3eAOCC approach is that the value of R computed without cascades (dotted black lines in Fig. 3), i.e., stemming from the genuine scattering $2p$ capture process alone, is found to lie between 0.9 and 1.5 for both targets. These results depart significantly from the two limits one can expect from spin statistics arguments, and indicate that all three levels are populated, in a nonstatistical way. This also shows that even in our high impact energy domain, i.e., for collision timescales of the order of 10^{-17} s (attosecond regime), the $1s2s$ projectile core electrons cannot be considered frozen, but that channel couplings and electronic correlations play a crucial role in determining the state populations created by the addition of the captured electron. Therefore, one-electron models describing simply the dynamics of the captured electron alone, cannot give a realistic view, though they may provide reasonable cross sections.

To gain further insight into the SEC dynamics [Eq. (1)], we consider the simplest representation of the three $1s2s2p$ ^4P, $^2P_\pm$ states in terms of the $1s$, $2s$, and $2p$ atomic orbitals, schematically represented only by their spins as

$$|^4P\rangle \equiv |\uparrow\uparrow\uparrow|, \tag{3a}$$

$$|^2P_-\rangle \equiv \frac{1}{\sqrt{2}}(|\uparrow\downarrow\uparrow| - |\downarrow\uparrow\uparrow|), \tag{3b}$$

$$|^2P_+\rangle \equiv \frac{1}{\sqrt{6}}(|\downarrow\uparrow\uparrow| + |\uparrow\downarrow\uparrow| - 2|\uparrow\uparrow\downarrow|) \tag{3c}$$

(see Supplemental Material [44]). These simple determinantal state wave functions are eigenfunctions of $\mathbf{S}^2$, the total spin operator, and correspond for simplicity here, to the largest M_S components. They do provide correct energy ordering of the states, as driven by the dominant exchange integral between $2s$ and $2p$ orbitals. Starting from the initial $1s2s\,^3S$ state ($\equiv\uparrow\uparrow$), a spin-up or -down target electron can be directly transferred to the projectile to create, respectively, the ^4P state [Eq. (3a)] or the $^2P_+$ state [through the third term in Eq. (3c)]. However, the creation of the $^2P_-$ state requires, in addition to transfer, a spin exchange between the active target electron and one of the projectile electrons. This involves a second-order process, less likely than the direct capture mechanism populating the ^4P and $^2P_+$ states. To support and further quantify this model, we estimate the relative magnitude of electron capture to these three levels using the Oppenheimer-Brinkman-Kramers (OBK) approximation [44,49]. Capture to the two favored levels, ^4P and $^2P_+$, is then described as dominantly driven by the projectile nucleus-electron attraction matrix element

I^P between the target $1s$ and the carbon $2p$ orbitals, i.e., I^P for ^{4}P and $\sqrt{2/3}I^P$ for ^{2}P$_+$ (see Supplemental Material [44]). However, capture to the ^{2}P$_-$ level is exclusively controlled by exchange electron-electron couplings, approximately a factor $Z_p = 6$ weaker.

This rather simple explanatory model, based on a correct spin and spatial description of the states, nevertheless gives a reasonable estimate of the ratio R, with an upper limit (neglecting the weak ^{2}P$_-$ capture contribution) equal to $3/2$, in agreement with our elaborate *ab initio* 3eAOCC calculations. It clearly exposes the weaknesses of frozen core approximations and pure spin statistics considerations and provides evidence for the existence of a sophisticated, counterintuitive [50] effect. This latter selectively bars direct capture to the ^{2}P$_-$, expected to be the only active doublet channel in the frozen core picture, by shielding the Coulomb attraction between the projectile nucleus and the active electron (no I^P coupling to promote this channel in OBK). This mechanism is only active when the Pauli exclusion principle can be advocated, i.e., in multielectron systems and approaches, and we therefore refer to it as Pauli shielding. This mechanism is clearly different from other Pauli excitation, exchange, and blocking mechanisms advocated in past investigations [7,21,51]. This simple explanatory model brings out all the physical features needed to interpret the outcome of the experiment. However, only configuration interaction and close coupling (included in 3eAOCC) can provide a quantitative description of the C^{3+} doubly excited states populated during the collision.

In conclusion, we provide experimental results for the $1s2s2p$ ^{4}P/^{2}P$_\pm$ line ratio R for single electron capture in fast collisions of $C^{4+}(1s2s\,^3\mathrm{S})$ with helium and hydrogen targets. Our measured R values are found to be nearly constant with collision energy and close to 2, in contrast to previous findings. In parallel, the ratio R calculated using a sophisticated multielectron close-coupling approach is found to be in agreement, for the first time, with experiment, when postcollisional radiative cascades are also taken into account. These results resolve the previously existing disagreement between theory and experiment and draw attention to the limited predictive power of the frozen core approximation as regards to spin statistics in highly correlated dynamical atomic systems. To better understand our findings, we propose an elegant Pauli shielding mechanism related to strong exchange effects which selectively (and counter intuitively) obstructs specific reaction channels. Systematic isoelectronic studies will be of great interest to further validate these conclusions in a more general context.

We thank Teck-Ghee Lee, Tom Kirchner, Tom Gorczyca, Steve Manson, and Anil Pradhan for helpful exchanges on various aspects of atomic structure, capture calculations, spin statistics, and cascades. We also thank the personnel of the "Demokritos" Tandem for their help with the experiment. We acknowledge support by the project "Cluster of Accelerator Laboratories for Ion-Beam Research and Applications—CALIBRA" (MIS 5002799) which is implemented under the Action "Reinforcement of the Research and Innovation Infrastructure," funded by the Operational Programme "Competitiveness, Entrepreneurship and Innovation" (NSRF 2014-2020) and co-financed by Greece and the European Union (European Regional Development Fund). T. J. M. Z. and A. D. also acknowledge support from the LABEX PLAS@PAR under Grant No. ANR-11-IDEX-0004-02.

*tzouros@physics.uoc.gr
†alain.dubois@sorbonne-universite.fr

[1] H. F. Beyer and V. P. Shevelko, *Introduction to the Physics of Highly Charged Ions*, Series in Atomic and Molecular Physics (Institute of Physics Publishing, Bristol and Philadelphia, 2003).
[2] A. K. Pradhan and S. N. Nahar, *Atomic Astrophysics and Spectroscopy* (Cambridge University Press, Cambridge, England, 2011).
[3] T. R. Kallman and P. Palmeri, Atomic data for x-ray astrophysics, Rev. Mod. Phys. **79**, 79 (2007).
[4] N. Stolterfoht, High resolution Auger spectroscopy in energetic ion atom collisions, Phys. Rep. **146**, 315 (1987).
[5] P. Beiersdorfer, Laboratory X-ray astrophysics, Annu. Rev. Astron. Astrophys. **41**, 343 (2003).
[6] *Atomic Processes in Basic and Applied Physics* edited by V. P. Shevelko and H. Tawara (Springer, Berlin Heidelberg, New York, 2012).
[7] W. Brandt and R. Laubert, Pauli Excitation of Atoms in Collision, Phys. Rev. Lett. **24**, 1037 (1970); K-shell ionization cross sections in asymmetric heavy-ion-atom collisions, Phys. Rev. A **11**, 1233 (1975).
[8] J. H. McGuire, N. Stolterfoht, and P. R. Simony, Screening and antiscreening by projectile electrons in high-velocity atomic collisions, Phys. Rev. A **24**, 97 (1981).
[9] T. J. M. Zouros, D. H. Lee, and P. Richard, Projectile $1s \rightarrow 2p$ Excitation Due to Electron-Electron Interaction in Collisions of O^{5+} and F^{6+} Ions with He and H_2 Targets, Phys. Rev. Lett. **62**, 2261 (1989).
[10] N. Stolterfoht, Time ordering of two-step processes in energetic ion-atom collisions: Basic formalism, Phys. Rev. A **48**, 2980 (1993).
[11] E. C. Montenegro, W. S. Melo, W. E. Meyerhof, and A. G. de Pinho, Separation of the Screening and Antiscreening Effects in the Electron Loss of He^+ on H_2 and He, Phys. Rev. Lett. **69**, 3033 (1992).
[12] Note, however, when considering capture involving hydrogenic ground state ions, the situation is clearer, as for example shown in high-resolution x-ray measurements [13,14], where spin statistics seem to be verified.
[13] F. Hopkins, R. L. Kauffman, C. W. Woods, and P. Richard, K x-ray transitions in one- and two-electron oxygen and fluorine projectiles produced in helium, neon, and argon targets, Phys. Rev. A **9**, 2413 (1974).

[14] M. Trassinelli, C. Prigent, E. Lamour, F. Mezdari, J. Mérot, R. Reuschl, J.-P. Rozet, S. Steydli, and D. Vernhet, Investigation of slow collisions for (quasi) symmetric heavy systems: What can be extracted from high resolution x-ray spectra, J. Phys. B **45**, 085202 (2012).

[15] T. R. Dillingham, J. Newcomb, J. Hall, P. L. Pepmiller, and P. Richard, Projectile K-Auger-electron production by bare, one-, and two-electron ions, Phys. Rev. A **29**, 3029 (1984); Erratum, Phys. Rev. A **32**, 1244(E) (1985).

[16] M. Zamkov, E. P. Benis, P. Richard, and T. J. M. Zouros, Fraction of metastable $1s2s\,^3S$ ions in fast He-like beams ($Z = 5$–9) produced in collisions with carbon foils, Phys. Rev. A **65**, 062706 (2002).

[17] E. P. Benis, I. Madesis, A. Laoutaris, S. Nanos, and T. J. M. Zouros, Mixed-state ionic beams: An effective tool for collision dynamics investigations, Atoms **6**, 66 (2018).

[18] Spin statistics arguments should strictly apply to energy *degenerate* states.

[19] E. P. Benis, T. J. M. Zouros, T. W. Gorczyca, A. D. González, and P. Richard, Elastic resonant and non-resonant differential scattering of quasifree electrons from $B^{4+}(1s)$ and $B^{3+}(1s^2)$ ions, Phys. Rev. A **69**, 052718 (2004); Erratum, Phys. Rev. A **73**, 029901 (2006).

[20] D. Strohschein, D. Röhrbein, T. Kirchner, S. Fritzsche, J. Baran, and J. A. Tanis, Nonstatistical enhancement of the $1s2s2p\,^4P$ state in electron transfer in 0.5–1.0-MeV/u $C^{4,5+}$ + He and Ne collisions, Phys. Rev. A **77**, 022706 (2008).

[21] J. A. Tanis, A. L. Landers, D. J. Pole, A. S. Alnaser, S. Hossain, and T. Kirchner, Evidence for Pauli Exchange Leading to Excited-State Enhancement in Electron Transfer, Phys. Rev. Lett. **92**, 133201 (2004); Erratum, Phys. Rev. Lett. **96**, 019901 (2006).

[22] T. J. M. Zouros, B. Sulik, L. Gulyás, and K. Tőkési, Selective enhancement of $1s2s2p\,^4P_J$ metastable states populated by cascades in single-electron transfer collisions of $F^{7+}(1s^2/1s2s\,^3S)$ ions with He and H_2 targets, Phys. Rev. A **77**, 050701 (2008).

[23] O. J. Kroneisen, H. J. Lüdde, T. Kirchner, and R. M. Dreizler, The basis generator method: Optimized dynamical representation of the solution of time-dependent quantum problems, J. Phys. A **32**, 2141 (1999).

[24] M. Zapukhlyak, T. Kirchner, H. J. Lüdde, S. Knoop, R. Morgenstern, and R. Hoekstra, Inner- and outer-shell electron dynamics in proton collisions with sodium atoms, J. Phys. B **38**, 2353 (2005).

[25] D. Röhrbein, T. Kirchner, and S. Fritzsche, Role of cascade and Auger effects in the enhanced population of the $C^{3+}(1s2s2p\,^4P)$ states following single-electron capture in $C^{4+}(1s2s\,^3S)$-He collisions, Phys. Rev. A **81**, 042701 (2010).

[26] J. W. Gao, Y. Wu, J. G. Wang, N. Sisourat, and A. Dubois, State-selective electron transfer in He^+ + He collisions at intermediate energies, Phys. Rev. A **97**, 052709 (2018).

[27] E. P. Benis and T. J. M. Zouros, Determination of the $1s2\ell2\ell'$ state production ratios $^4P^o/^2P$, $^2D/^2P$ and $^2P_+/^2P_-$ from fast $(1s^2, 1s2s\,^3S)$ mixed-state He-like ion beams in collisions with H_2 targets, J. Phys. B **49**, 235202 (2016).

[28] E. P. Benis, I. Madesis, A. Laoutaris, S. Nikolaou, A. Dubois, T. W. Gorczyca, and T. J. M. Zouros, Population of the $1s2s(^3S)nl\,^2L$ states in collisions of mixed-state $(1s^2\,^1S, 1s2s\,^3S)$ B^{3+} and C^{4+} ion beams with He/H_2 targets, X-Ray Spectrom. **49**, 54 (2020).

[29] T. J. M. Zouros and D. H. Lee, in *Accelerator-Based Atomic Physics: Techniques and Applications*, edited by S. M. Shafroth and J. C. Austin (AIP, Woodbury, NY, 1997), pp. 426–479.

[30] I. Madesis, A. Laoutaris, T. J. M. Zouros, S. Nanos, and E. P. Benis, in *State-of-the-Art Reviews on Energetic Ion-Atom and Ion-Molecule Collisions*, Interdisciplinary Research on Particle Collisions and Quantitative Spectroscopy Vol. 2, edited by D. Belkić, I. Bray, and A. Kadyrov (World Scientific, Singapore, 2019), pp. 1–31.

[31] E. P. Benis, T. J. M. Zouros, H. Aliabadi, and P. Richard, Hemispherical analyser with 2-D PSD for zero-degree Auger projectile spectroscopy, Phys. Scr. **T80B**, 529 (1999).

[32] D. H. Lee, P. Richard, J. M. Sanders, T. J. M. Zouros, J. L. Shinpaugh, and S. L. Varghese, Electron capture and excitation studied by state-resolved KLL Auger measurement in 0.25–2 MeV/u $F^{7+}(1s^2\,^1S, 1s2s\,^3S) + H_2/He$ collisions, Nucl. Instrum. Methods Phys. Res., Sect. B **56–57**, 99 (1991).

[33] T. J. M. Zouros, *Resonant transfer and excitation associated with Auger electron emission, in Recombination of Atomic Ions*, NATO Advanced Study Institute Series B: Physics Vol. 296, edited by W. G. Graham, W. Fritsch, Y. Hahn, and J. Tanis (Plenum Publishing Corporation, New York, 1992), pp. 271–300.

[34] D. H. Lee, P. Richard, J. M. Sanders, T. J. M. Zouros, J. L. Shinpaugh, and S. L. Varghese, KLL resonant transfer and excitation to $F^{6+}(1s2l2l')$ intermediate states, Phys. Rev. A **44**, 1636 (1991).

[35] S. Doukas, I. Madesis, A. Dimitriou, A. Laoutaris, T. J. M. Zouros, and E. P. Benis, Determination of the solid angle and response function of a hemispherical spectrograph with injection lens for Auger electrons emitted from long lived projectile states, Rev. Sci. Instrum. **86**, 043111 (2015).

[36] E. P. Benis, I. Madesis, A. Laoutaris, S. Nanos, and T. J. M. Zouros, Experimental determination of the effective solid angle of long-lived projectile states in zero-degree Auger projectile spectroscopy, J. Electron Spectrosc. Relat. Phenom. **222**, 31 (2018).

[37] E. P. Benis, S. Doukas, T. J. M. Zouros, P. Indelicato, F. Parente, C. Martins, J. P. Santos, and J. P. Marques, Evaluation of the effective solid angle of a hemispherical deflector analyser with injection lens for metastable Auger projectile states, Nucl. Instrum. Methods Phys. Res., Sect. B **365**, 457 (2015).

[38] S. Mannervik, Optical studies of multiply excited states, Phys. Scr. **40**, 28 (1989).

[39] C. Laughlin, Calculations on transitions in singly- and doubly-excited C IV, Z. Phys. D **9**, 273 (1988).

[40] L. Guillemot, P. Roncin, M. N. Gaboriaud, M. Barat, H. Laurent, S. Bliman, M. G. Suraud, D. Hitz, M. Bonnefoy, A. Chassevent, and A. Fleury, Collisions of metastable He-like C^{4+} ions on He and H_2 targets, J. Phys. B **23**, 3353 (1990).

[41] N. Sisourat, I. Pilskog, and A. Dubois, Non perturbative treatment of multielectron processes in ion-molecule scattering: Application to He^{2+}-H_2 collisions, Phys. Rev. A **84**, 052722 (2011).

[42] N. Sisourat and A. Dubois, in *Semiclassical close-coupling approaches, in Ion-Atom Collision—The Few-Body Problem in Dynamics Systems*, edited by M. Schultz (de Gruyter, Berlin/Boston, 2019), pp. 157–177.

[43] The He target is described by a model potential binding just a single electron [44].

[44] See Supplemental Material at http://link.aps.org/supplemental/10.1103/PhysRevLett.124.113401, for additional details and discussions on the theoretical approach including 3eAOCC and simplified static and dynamic models. It includes Refs. [45,46].

[45] M. H. Chen, Dielectronic satellite spectra for He-like ions, At. Data Nucl. Data Tables **34**, 301 (1986).

[46] P. D. Dumont, H. P. Garnir, Y. Baudinet-Robinet, and K. T. Chung, Quartet system of C IV, Phys. Rev. A **32**, 229 (1985).

[47] However, and as a supplementary support of the present results, we note that the previous independent R measurements (Ref. [20], red circles in Fig. 3) have been recently reevaluated [36] by proper $\overline{G_\tau}$ corrections to $R \simeq 2$, a value in agreement with our data.

[48] R. D. Cowan, *The Theory of Atomic Structure and Spectra* (University of California Press, Berkeley, CA, 1981).

[49] M. R. C. McDowell and J. P. Coleman, *Introduction to the Theory of Ion-Atom Collisions* (North-Holland Publishing Co., New York, 1970).

[50] In a pure frozen core picture, the capture of a spin-down electron to the lower energy level of the $1s2s$ configuration (i.e., our initial ^{3}S state) should intuitively lead to the production of the *lower* energy $1s2s2p$ ^{2}P state, symbolized here by ^{2}P_ (a spin-up electron can produce only the ^{4}P state). However, in the model using Eqs. (3) (see also Supplemental Material [44]), the OBK treatment gives rise to a negligibly small cross section for that ^{2}P_, which is counterintuitive according to the pure frozen core picture. In our model, this process is blocked by Pauli shielding as stated in the manuscript.

[51] N. Stolterfoht, A. Mattis, D. Schneider, G. Schiwietz, B. Skogvall, B. Sulik, and S. Ricz, Time-ordering effects in K-shell excitations of 170-MeV Ne^{7+} colliding with gas atoms: Single excitation, Phys. Rev. A **48**, 2986 (1993).